Dynamic Global Potentials and Second Virial Coefficients from Trajectory Calculations

Victor Bernshtein and Izhack Oref*

Department of Chemistry, Technion-Israel Institute of Technology, Haifa 32000, Israel

Received: September 27, 1999; In Final Form: November 17, 1999

We report on a novel method of verifying the validity of intermolecular potentials. By using trajectory calculations with an ab initio pairwise potential or an assumed Lennard-Jones pairwise potential, we calculate the intermolecular dynamic global potential which can be used to calculate experimentally obtained quantities such as a second virial coefficient. The agreement between calculated and experimental quantities is a measure of the quality of the intermolecular potential that is used in such calculations. The method is demonstrated for benzene−Ar collisions. An ab initio and a Lennard-Jones pairwise potentials are used, and calculations of the dynamic global potential and the second virial coefficient were performed at 300, 700, 1500, and 2820 K. It is found that the dynamic global potential is a function of the temperature, and explanations which take into consideration the anisotropic potential of the benzene molecule and the effects of the vibrational, rotational, and translational energies on the dynamic global potential are provided. The method applies to neat gases as well as to binary gas mixtures.

Introduction

Many physical properties of gases depend on details of the intermolecular potential that are largely unknown. Therefore, parameters in empirical or calculated potentials are adjusted until agreement is obtained with experimental data such as viscosity, thermal conductivity, or the second virial coefficient ($B(T)$).[1−9] (There is extensive literature on the subject and additional references can be found in refs 1 and 3−9.) The pragmatic way by which empirical potential parameters can be obtained from $B(T)$, defined by the equation

$$pV/RT = 1 + B(T)/V + C(T)/V^2 + ... \qquad (1)$$

is by systematic iterations until a reasonable agreement between calculated and experimental $B(T)$ is obtained. Such procedures sometimes give unphysical results. Thus, the unphysical square-well potential yields good agreement with experimental values of $B(T)$, while a LJ or a Sutherland potential gives poor results.[2]

Early work used simple empirical potentials such as Lennard-Jones (LJ), Kihara, exp-6, Sutherland, square well, and others[1,2] to calculate $B(T)$. More recently, advanced computational methods were used to obtain intermolecular potentials.[3−9] Atomic force field calculations were used to calculate $B(T)$ as well as thermodynamic properties of gas phase and liquid benzene.[3] It turns out that, in spite of the good agreement between experiment and calculations of the values of $B(T)$ in the gas phase, only specific force fields gave a good agreement with liquid-phase results as well.[3] This is due to the averaging effect of all the orientations in gas-phase binary collisions that is absent in the liquid phase.[3] Good agreement of some force fields with quantum calculations is obtained. Empirical potential energy surfaces (PES) for nonvibrating mixed gases, Ar−CO_2, were obtained by a least-square fitting to high-resolution spectra of van der Waals complexes and to $B(T)$.[4] Rotation and quantum corrections were used in the calculations of $B(T)$. Here again, a variety of different PES gave a good agreement with experimental values of $B(T)$. Another approach is to use perturbation theory with reduced parameters.[5] This is a pragmatic approach which yields potentials for neat gases and gas mixtures. The potentials that are obtained by this approach are basically static potentials.

Ab initio calculations were done on uracil dimers using an empirical potential and a rigid rotor−harmonic oscillator−ideal gas approximation.[6] Since, in this method, the number of degrees of freedom is limited, direct numerical integration to obtain $B(T)$ was performed. A potential of mean force is used in conjunction with assumed potentials to obtain $B(T)$.[7] Here again, different potentials yield the same value of $B(T)$. The potential parameters for alkanes were found by using force field calculations and a potential fitting to experimental values of $B(T)$.[8] For polyatomic molecules the situation is even more complicated. The internal vibrational−rotational energies affect the kinetic parameters in a complicated way, making direct correlation between intermolecular potential and experimental kinetic data an extremely complicated task. In our trajectory calculation approach, reported in the next sections, we calculate $B(T)$ for a mixed gas of an atom and a polyatomic molecule with fully active vibrations and rotations.

Lately, quasiclassical trajectory−molecular dynamics calculations are used to explore binary molecular collisions and chemical reactions.[10−31] Specifically, molecular dynamics calculations are used to obtain quantities such as average energy transferred per collision,[22,23,27,31b] $\langle \Delta E \rangle$, energy transfer probability density functions, $P(E',E)$,[31] reactions rate coefficients,[31b] and lifetimes.[23] These trajectory calculations use pairwise empirical[22,23] or fitted ab initio pairwise intermolecular potentials[31] that are obtained by various recipes.[33] For example, one empirical procedure is to use a pairwise LJ potential and adjust the values of ϵ_i and σ_i pairwise parameters by additional parameters that are derived from the global LJ parameters.[22] Ab initio PES require fitting and adjustments as well to convert them to a pairwise form that is useful for practical calculations.[33] The sum of all pairwise potentials for an atom approaching a molecule in a given, fixed direction in space yields a static global

* Corresponding author. E-mail: chroref@aluf.technion.ac.il.

10.1021/jp993451i CCC: $19.00
Published on Web 01/11/2000

potential. These static potentials are not useful in the calculations of experimental results for reasons that are described below.

In a recent paper[31] we have developed a method that enables the calculations of an average, or a global, dynamic potential by averaging many single-trajectory potentials. A dynamic global potential is not only instructive, it is also useful, since it represents a quantity that is based on averaging tens of thousand of trajectories with all possible orientations and impact parameters. It can be used, for example, to calculate $B(T)$. It is possible then to compare calculations with experiments. Dynamic global potentials are obtained by binning the potential energy as a function of the center-of-mass (CM) distance for all the trajectories and dividing the sum in each bin by the number of times the atom traverses the given CM distance that is represented by a particular bin. Monte Carlo sampling of impact parameters and Euler's angles is used. This method is especially useful for nonspherical molecules with an anisotropic potential like benzene.[31] The dynamic global potential, which is obtained that way, has a complicated shape and cannot be fit to any simple equation.[31] A spherical, or a static, potential simply would not do.

In principle, inversion of $B(T)$ yields intermolecular potentials. However, inversions are impractical and in the rarest of cases, when the procedure applies, the results are not unique.[1] More than one potential can be obtained.[1−8] Therefore, reliable pairwise potentials remain one of the pressing problems of molecular dynamics. In the following, we show how starting from pairwise potentials it is possible to obtain $B(T)$ and thus verify experimentally the validity of an intermolecular potential.

Theory

The numerical methods used in the present work are reported in refs 23 and 24. The equations of motion are integrated by using a modified public domain program Venus.[32] The intermolecular potential is pairwise fitted ab initio[33] or Lennard-Jones potentials. Bludsky, Spirko, Herouda, and Hobza,[33] BSHH, have reported ab initio calculations of an Ar−benzene cluster and fitted the results to a potential function which contains pairwise atom−atom interactions. This is called the BSHH potential.

$$V_{ij} = \frac{A_{ij}}{r_{ij}^{\alpha}} - B_{ij}\left(\frac{1}{r_{ij}^{6}} - \frac{C_{ij}}{r_{ij}^{7}}\right); \qquad i,j = 1-6 \tag{2}$$

A, B, and C are constants, r is the CM relative distance, i indicates a carbon or a hydrogen atom, and j indicates an argon atom. The LJ parameters were evaluated by the method of ref 22 and are given in ref 27. Basically, the well-depth ϵ and the collision radius σ of the pairwise C−Ar and H−Ar LJ interactions are given by the Ne−Ar and the He−Ar values, respectively, calculated by the normal combination rules. The parameters of the potential are then adjusted to give the overall effective ϵ and σ values.

The intramolecular potential includes all the normal mode contributions, stretching, bending, and wagging. The values of the parameters of this potential were obtained from the modified valance force field calculations by Draeger[34] and are given also in refs 23 and 24. The initial translational and rotational energies were chosen from the appropriate thermal energy distributions. The initial impact parameter was chosen randomly from values between 0 and its maximum value b_m. The initial internal energy was either the average thermal energy or an assigned value. The energy was distributed statistically among all the normal modes of the molecule. The value of the maximum impact parameter b_m was determined separately.[23,24] A value of 0.9 nm was used in the present calculations. A total of 30 000−50 000 trajectories were used in the present study for each dynamic global potential. The large number of trajectories was chosen to provide good statistical sampling in the binning process.

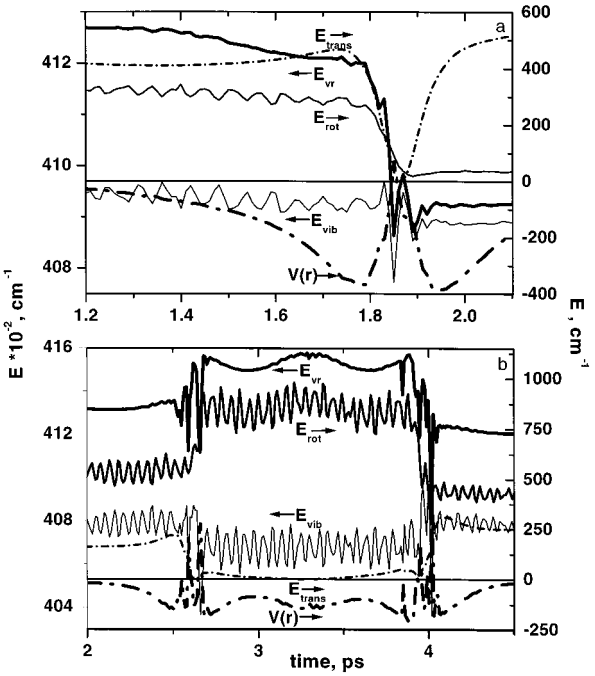

Figure 1. Energy vs time of individual trajectories. The arrows indicate left or right coordinate. (a) A short duration trajectory. The atom approaches the center of mass in a perpendicular direction to the plane of the molecule. (b) A long duration trajectory. The atom approaches in the plane of the molecule.

The second virial coefficient is defined by the equation

$$B(T) = 2\pi N_A \int_0^{\infty} (1 - \exp(-V(r)/kT) r^2 \, dr \tag{3}$$

where $V(r)$ is the dynamic intermolecular global potential and r is the separation between the centers of mass of the colliding pair. The reduced virial coefficient, $B^*(T^*)$, is defined by

$$B^*(T^*) = B(T)/b_0 \tag{4}$$

where T^* is the reduced temperature, $T^* = kT/\epsilon$, k is Boltzmann's constant, and ϵ is the well-depth. The value of b_0 is $2\pi N_A \sigma^3/3$. N_A is Avogadro's number and σ is the distance between the molecular centers when the potential is zero. This definition applies to cases, like the present one, where the intermolecular potential is anisotropic.

The methodology of evaluating $B(T)$ is as follows. The values of the dynamic global potential from the trajectory calculations are placed directly in eq 3. No smoothing or data reduction is performed. Extrapolation of the data is done at very short and very long distances outside the trajectory's effective range. This way integration is performed from near zero to very long distances.

Results and Discussion

The dynamic global intermolecular potential is a result of averaging 30 000−50 000 trajectories. Each trajectory has its particular time evolution. Figure 1 shows two trajectories. Each graphical representation of a trajectory exhibits a time evolution of the vibrational, translational, rotational, and the intermolecular potential as a function of time. The rotational and translational

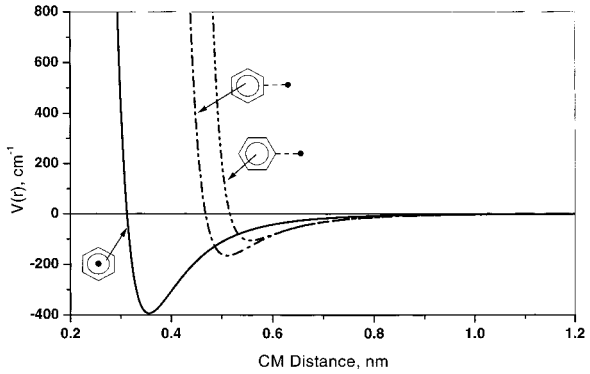

Figure 2. Static global potentials vs center-of-mass distance calculated by using BSHH ab initio pairwise potential. The full circle indicates an Ar atom. (−) Ar on top of the center of the benzene ring. (-·-) The Ar in the plane of the molecule on a line connecting the center-of-mass of the molecule and the center of the C−C bond. (-··-) The Ar in the plane of the molecule on a line connecting the center-of-mass of the molecule and the C−H bond.

energies were chosen randomly from the appropriate Boltzmann distributions. As can be seen, the intermolecular potential changes greatly at the point of impact. The Ar atom climbs on the repulsive wall and the potential energy increases. The same process occurs at the end of the collision. In between, there is a change in the potential energy as the atom samples parts of the molecular space.

Single Trajectories. Figure 1a shows a trajectory of a collision of very short duration, 150 fs. The atom hits the molecule and climbs the repulsive wall; then the relative translational energy drops to zero and increases to its final value as the pair separate. During the collision, the molecule lost its rotational energy, while there was hardly any change in the vibrational energy. This is a classical case of R → T energy transfer process. This trajectory describes a down collision with $\Delta E = -325$ cm^{-1}. The depth of the potential well indicates that the atom approaches the molecule from above its center of mass. This can be seen from the static potentials in Figure 2. The static potential is obtained by summing up all pairwise potentials when the atom approaches the nonrotating molecule from a given direction. When the atom approaches the molecule in a perpendicular direction to the plane of the molecule, the minimum in the potential is deeper and at a shorter distance than when the atom approaches from any other direction. The well-depth of 400 cm^{-1} of the trajectory in Figure 1a corresponds exactly to the deepest well in the static potential, namely, the Ar above the CM of the benzene.

Figure 1b shows a trajectory of a long-lived collision. The Ar atom hovers over the molecule for a long time, 1500 fs. During the collision lifetime there is a constant exchange of vibrational−rotational energies while the translational energy is, practically, zero. At the end of the collision the atom climbs the repulsive wall and it is "kicked" out. Here again the energy transfer is mostly R → T and $\Delta E = -113$ cm^{-1}. From the potential well-depth (see Figure 2) we know that the initial atom-molecule collision occurred when the atom was in the plane of the molecule. An analysis of many single trajectories indicates that the atom does not stay at its initial impact location but samples various parts of the molecular space.

The value of the potential energy at each intermolecular distance in each trajectory is sampled and binned, and an average of the potential energy of all the trajectories at each bin is taken. The final outcome is a dynamic global potential averaged over all orientations of the nonsymmetric molecule and averaged over

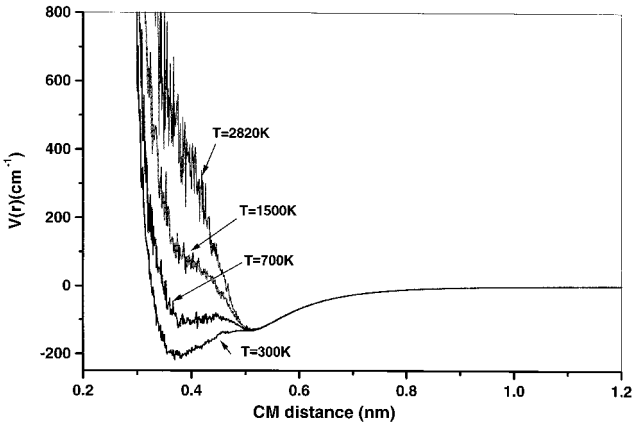

Figure 3. Dynamic global potentials vs center-of-mass distance. ∼40 000 trajectories averaged over all initial conditions were used. These potentials are based on BSHH ab initio pairwise potential.

Boltzmann distributions of translational, vibrational, and rotational energies at a given temperature.

Global Potential. The dynamic global potentials, which are based on a BSHH ab initio pairwise potential, at four temperatures are given in Figure 3. The general features of the curves are totally different. At 2820 K the curve resembles a spherical molecule with a minimum at 0.517 nm. The reason for that is that the approaching Ar atom "sees" a fast rotating molecule that is basically a rotating sphere. The distance at zero potential energy is 0.467 nm, not much different from the Lennard-Jones effective $\sigma_{\text{benzene-Ar}} = 0.447$ nm reported in the literature.[25] The similarity of the values is not surprising since the effective σ is evaluated for a spherical potential. The corrected cross section is given by the expression $\sigma^2_{\text{cor}} = \Omega^{(2,2)*}\sigma^2$ where $\Omega^{(2,2)*}$ is the reduced collision integral. The value of σ_{corr} is 0.37 nm. The correction clearly does not improve the value of σ. The LJ based collision integral is not a good correction for the anisotropic system that is studied here.

The low-temperature dynamic global potential has a totally different shape. The minimum in the curve is deeper and at a shorter CM distance, 0.38 nm. The point of zero potential is at 0.327 nm, much shorter than the high temperature case and much different than the value of $\sigma_{\text{benzene-Ar}}$ quoted above. The dynamic global potential shows also an irregularity in the range ∼0.46−0.517 nm. The upper value is the location of the minima of the dynamic global potentials at higher temperatures. The reasons for the differences between the high-temperature and low-temperature global potentials can be explained as follows. At low temperatures the asymmetry of the benzene comes into play. This can be seen from the static potentials in Figure 2. At low temperatures, the slow rotations and low translational energies enable the atom to find its way to the deepest potential well, which is located above the CM of the molecule.[31] Therefore, a deep well is expected in the dynamic global potential at about the same distance as the minimum in the static global potential. The irregularity in the dynamic global potential is also due to the anisotropic potential of the benzene molecule. The reason is that the other shallower wells in the potential energy surface appear at larger distances as can be seen from the static potential shown in Figure 2. Therefore, short CM distances are excluded when the Ar approaches in the plane of the molecule because the nearest CM distance must be longer than the CM−hydrogen atom distance or the distance between the CM and the center of the C−C bond (Figure 2). The irregular shape of the dynamic global potential precludes a simple fitting equation in the CM coordinate system. (In the distance of closest

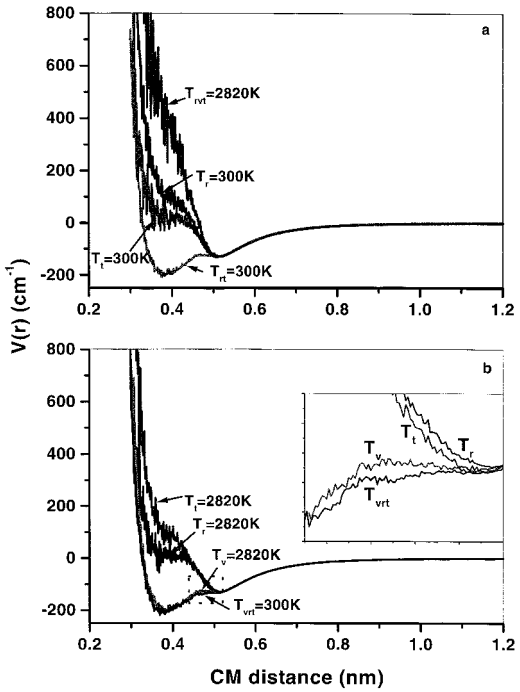

Figure 4. Dynamic global potentials vs center-of-mass distance. ~40 000 trajectories averaged over all initial conditions were used. These potentials are based on BSHH ab initio pairwise potential. T_r indicates rotational temperature. T_t indicates translational temperature. T_v indicates vibrational temperature. (a) The temperatures of all the modes are 2820 K except as indicated. (b) The temperatures of all the modes are 300 K except as indicated. The enlargement of the barred rectangle is in the insert. It shows that there is hardly any difference between T_v and T_{vrt}. The vertical scale in the insert is from −180 to −80 cm^{-1}. The horizontal scale is from 0.42 to 0.52 nm.

approach, minimal distance, coordinate system the global potential is regular and can be fit to an exp-r^{-6} potential.[31])

The dynamic global potentials at 700 and 1500 K are also shown in Figure 3. As expected, these potentials are intermediate cases between the high- and the low-temperature cases. The 700 K curve shows a double-minima potential. The first is at the location of the minimum of the 300 K curve, and the second at the location of the minimum of the 2820 K curve. The first minimum is shallower than the minimum at 300 K, because the molecule rotates faster and collisions occur, on the average, at larger distances. This manifests itself in a larger value for σ, which is 0.348 nm compared with the distance of zero potential of 0.327 nm at 300 K. The 1500 K curve has one minimum only at the same position as the second minimum of the 700 K curve and at the same position of the minimum of the 2820 K curve. Instead of the first minimum there is an inflection point. The explanation for the different shapes of the potential curves is, in a nutshell, that at high temperatures the fast rotations expose a spherical molecule to the high-velocity incoming atom. The collision duration is short[23] and the atom does not sample the whole PES. At low temperatures, the slow rotations and translations enable the atom to sample a greater part of the PES. In the next section we check this point in detail.

Effects of Vibrational, Rotational, and Translational Energies on the Shape of the Potential Curve. To test the effects of vibrational, v, rotational, r, and translational, t, energies on the dynamic global potential we ran sets of 30 000 trajectories with different initial conditions, and Figure 4 shows the results. Four curves are shown in Figure 4a. One is when the system, e.g., vrt, is at a thermal equilibrium at 2820 K. Another curve is when v and t are at 2820 K and r is at 300 K. The rotationally cold molecule allows the fast moving atom to sample various parts of the PES and the global potential resembles the potential of a colder system. Next is a dynamic global potential curve for v and r at 2820 K and t at 300 K. Here the effect on the shape is even more dramatic. The low relative translational energy allows the atom to sample more of the PES and the curve resembles even more a low-temperature case. When both r and t are at 300 K but v is at 2820 K, the potential curve is almost identical to a canonical case where vrt are at 300 K. That is to say, vibrational excitation has practically no effect on the dynamic global potential. This stands to reason, since increasing the vibrational energy does not change the size of the molecule in any significant way, neither does it change the mechanism of the collision as do r and t.

Figure 4b reinforces the conclusions that were obtained from Figure 4a. It shows four dynamic global potentials. The thermal system is at 300 K and the temperature of one type of degree of freedom is changed systematically to 2820 K. A change in vibrational energy hardly changes the dynamic global potential. A change in rotational or translational energies has a profound effect on the potential. As before, translations have a larger effect than rotations.

Second Virial Coefficient. Values of $B(T)$ for various potentials and limiting conditions at four temperatures are given in Table 1. The calculations were performed over a wide temperature range. The temperatures studied were 300, 700, 1500, and 2820 K. Group 1 of numbers in Table 1 gives values of $B(T)$ that were obtained by placing the numerical values of the BSHH dynamic global potential, depicted in Figure 3, in eq 3. The integration is from 0 to ∞ and the potential at short distances, the repulsive part of the potential, and at long distances is obtained by extrapolation. Also given in this group of numbers are values of ϵ and σ that were obtained directly from the BSHH dynamic global potential, which is depicted in Figure 3. Comparisons of values of $B(T)$ in group 1 with values of $B(T)$ obtained from a LJ potential of identical σ and ϵ, group 3, and with values of $B(T)$ that were obtained from a LJ potential with literature values of σ and ϵ, group 4, show that the values of $B(T)$ in group 1 are markedly different. The spherical LJ potentials cannot reproduce accurately the values of $B(T)$ obtained from the BSHH dynamic global potential.

A more sensible way of calculating $B(T)$ from an ab initio potential is to integrate $V(r)$ in eq 3 starting from the atom−molecule distance of closest approach, $r_{initial}$ instead of integrating from $r = 0$. This way, the core dimensions and the excluded volume are taken into consideration. This is similar to the distance parameter in the Kihara potential[35] that replaces r by $r - r_{initial}$. Values of $B(T)$ that were calculated in this way are presented in group 2 together with the values of $r_{initial}$.

For comparison we have calculated $B(T)$ from a Kihara potential (which is given by eq 5) with identical values of ϵ

$$V(r) = 4\epsilon\left[\left(\frac{\sigma - r_{initial}}{r - r_{initial}}\right)^{12} - \left(\frac{\sigma - r_{initial}}{r - r_{initial}}\right)^{6}\right] \qquad (5)$$

and σ as in the calculations of $B(T)$ in groups 1 and 2. This information is given in group 6 in Table 1. The Kihara potential, which is basically a modified LJ potential, does not reproduce satisfactorily the values of $B(T)$ that were obtained from the BSHH dynamic global potential, even though the same ϵ and σ were used in both calculations.

We have also calculated a LJ dynamic global potential by running 30 000 trajectories using a LJ pairwise potential whose parameters are based on the literature values of σ and ϵ that

TABLE 1: Second Virial Coefficients for BSHH and Lennard-Jones Potentials as a Function of Temperature

1. $B(T)$ Calculated with a BSHH Potential (Integration from $r = 0$)

T, K	T^*	$B(T)$, cm^3 mol^{-1}	$B(T)^*$	σ, nm	ϵ, cm^{-1}
300	1.04	$-0.259\,99 \times 10^3$	$-0.584\,16 \times 10^1$	0.328[a]	201[a]
700	3.74	$-0.482\,86 \times 10^2$	$-0.916\,28$	0.347	130
1500	8.02	$0.126\,92 \times 10^2$	$0.113\,42$	0.446	130
2820	15.08	$0.332\,48 \times 10^2$	$0.258\,83$	0.467	130

2. $B(T)$ Calculated with a BSHH Potential (Integration from $r_{initial}$)

T, K	T^*	$B(T)$, cm^3 mol^{-1}	$B(T)^*$	σ, nm	ϵ, cm^{-1}	$r_{initial}$, nm
300	1.04	$-0.293\,89 \times 10^3$	$-0.660\,32 \times 10^1$	0.328[a]	201[a]	0.299
700	3.74	$-0.801\,47 \times 10^2$	$-0.152\,09 \times 10^1$	0.347	130	0.294
1500	8.02	$-0.159\,29 \times 10^2$	$-0.142\,36$	0.446	130	0.284
2820	15.08	$0.486\,82 \times 10^1$	$0.378\,98 \times 10^{-1}$	0.467	130	0.285

3. $B(T)$ Calculated with a LJ Potential (Integration from $r = 0$)

T, K	T^*	$B(T)$, cm^3 mol^{-1}	$B(T)^*$	σ, nm	ϵ, cm^{-1}
300	1.04	$-0.105\,89 \times 10^3$	$-0.237\,93 \times 10^1$	0.328[a]	201[a]
700	3.74	$0.366\,95 \times 10^1$	$0.696\,33 \times 10^{-1}$	0.347	130
1500	8.02	$0.463\,41 \times 10^2$	$0.414\,15$	0.446	130
2820	15.08	$0.656\,44 \times 10^2$	$0.511\,02$	0.467	130

4. $B(T)$ Calculated with a LJ Potential. σ(LJ) = 0.447 nm, ϵ(LJ) = 148 cm^{-1} from Our Work (Integration from $r = 0$)

T, K	T^*	$B(T)$, cm^3 mol^{-1}	$B(T)^*$
300	1.41	$-0.153\,01 \times 10^3$	$-0.135\,83 \times 10^1$
700	3.29	$-0.361\,91 \times 10^1$	$-0.321\,27 \times 10^{-1}$
1500	7.05	$0.425\,97 \times 10^2$	$0.378\,14$
2820	13.25	$0.562\,69 \times 10^2$	$0.499\,51$

5. $B(T)$ Calculated with a LJ Potential with σ_{corr} and ϵ(LJ) = 148 cm^{-1} (Integration from $r = 0$)

T, K	T^*	$B(T)$, cm^3 mol^{-1}	$B(T)^*$	σ_{corr}, nm
300	1.41	$-0.240\,86 \times 10^3$	$-0.135\,82 \times 10^1$	0.520
700	3.29	$-0.371\,68 \times 10^1$	$-0.321\,24 \times 10^{-1}$	0.520
1500	7.05	$0.631\,82 \times 10^2$	$0.564\,66$	0.520
2820	13.25	$0.765\,54 \times 10^2$	$0.595\,95$	0.397

6. $B(T)$ Calculated with a Kihara Potential (Eq 5) (Integration from $r_{initial}$)

T, K	T^*	$B(T)$, cm^3 mol^{-1}	$B(T)^*$	σ, nm	ϵ, cm^{-1}
300	1.04	$0.333\,01 \times 10^1$	$0.748\,22 \times 10^{-1}$	0.328[a]	201[a]
700	3.74	$0.155\,78 \times 10^2$	$0.295\,62$	0.347	130
1500	8.02	$0.631\,82 \times 10^2$	$0.564\,66$	0.446	130
2820	15.08	$0.765\,54 \times 10^2$	$0.595\,95$	0.467	130

7. $B(T)$ from a LJ Global Potential Obtained from a LJ Pairwise Potential with $\sigma = 0.286$ nm and $\epsilon = 508$ cm^{-1}

T, K	T^*	$B(T)$, cm^3 mol^{-1}	$B(T)^*$
300	0.41	$-0.826\,79 \times 10^3$	$-0.280\,22 \times 10^2$

[a] ϵ and σ were taken from the BSHH potential of Figure 3.

were calculated by the normal combination rules. Details are given in the theory section. The results for 300 K are given in group 7 in Table 1. The value of σ from the LJ dynamic global potential is 0.286 nm and the value of ϵ is 508 cm^{-1}. These values are to be compared with the literature values of σ and ϵ of 0.477 nm and 148 cm^{-1}, respectively. The values of $B(T)$ also differ by more than a factor of 5. That is to say, starting with a LJ pairwise potential that is based on literature values does not yield back a dynamic global potential or a virial coefficient that is obtained from literature values of a static LJ potential. We have also checked whether the values of $B(T)$ in group 4 improve by correcting the value of σ by the collision integral. The new values of $B(T)$ are given in group 5. We find that using a LJ potential with σ_{corr} does not improve the values of $B(T)$, and there are still large deviations from the values of $B(T)$ in group 1.

Refson et al.[36] reported differences of 8−10% in the values of $B(T)$ of water when flexible intramolecular potentials, instead of rigid potentials, are used. These findings support the validity of the present work, which uses flexible intramolecular potential for the benzene molecule. However, we would expect smaller deviations in the values of $B(T)$ of benzene when rigid and flexible potentials are used because the benzene molecule is structurally rigid. On the other hand, nonrigidity effects are expected to be more pronounced in water, which is a nonrigid molecule. The shape of the dynamic potential, which is affected very little by vibrational excitation, supports this conclusion.

In conclusion, it is possible, by using quasiclassical trajectory calculations, to verify the parameters of an intermolecular pairwise potential by calculating a dynamic global potential that can be used to check for an agreement between calculated and experimental quantities such as second virial coefficients. This approach is especially important for nonspherical systems with anisotropic potential where the static potential is orientation dependent and the dynamic global potential is not a smooth function of the relative center of mass distance. A comparison of the values of the second virial coefficient that were obtained from ab initio-based dynamic global potential with values that were calculated by using a Lennard-Jones and a Kihara empirical models shows a great discrepancy and points to the inadequacy of simple empirical models.

Acknowledgment. We thank K. F. Lim for his comments and the TRACS program and the Edinburgh Parallel Computing Center for providing computational facilities. This work is supported by the Fund for the Promotion of Research at the Technion, by the B. and N. Ginsburg Energy Research Fund, and by the Ministry of Science and the Arts.

References and Notes

(1) Maitland, G. C.; Rigby, M.; Smith, E. B.; Wakeham, W. A. *Intermolecular Forces*; Clarendon Press: Oxford, 1981.
(2) Sherwood, A. E.; Prausnitz, J. M. *J. Chem. Phys.* **1964**, *41*, 429.
(3) Smith, G. D.; Jaffe, R. L. *J. Phys. Chem.* **1996**, *100*, 9624.
(4) Hutson, J. M.; Ernesti, A.; Law, M. M.; Roche, C. F.; Wheatley, R. J. *J. Chem. Phys.* **1996**, *105*, 9130.
(5) Friedrich, A.; Lustig, R. *J. Chem. Phys.* **1996**, *105*, 9597.
(6) Kratochvil, M.; Engkvist, O.; Sponer, J.; Jungwirth, P.; Hobza, P. *J. Phys. Chem. A* **1998**, *102*, 6921.
(7) McCoy, J. D.; Curro, J. G. *Macromolecules* **1998**, *31*, 9362.
(8) Rodriguez, A. L.; Vega, C.; Freire, J. J. *J. Chem. Phys.* **1999**, *111*, 438.
(9) Fernández-Prini, R.; Japas, M. L. *J. Chem. Phys.* **1986**, *85*, 2951.
(10) Date, N.; Hase, W. L.; Gilbert, R. G. *J. Phys. Chem.* **1984**, *88*, 5135.
(11) Brown, N. J.; Miller, J. A. *J. Chem. Phys.* **1984**, *80*, 5568.
(12) Bruehl, M.; Schatz, G. C. *J. Chem. Phys.* **1998**, *89*, 770.
(13) Bruehl, M.; Schatz, G. C. *J. Phys. Chem.* **1988**, *92*, 7223.
(14) Lendvay, G.; Schatz, G. C. *J. Phys. Chem.* **1990**, *94*, 8864.
(15) Clarke, D. L.; Thompson, E. G.; Gilbert, R. G. *Chem. Phys. Lett.* **1991**, *182*, 357.
(16) Lendvay, G.; Schatz, G. C. *J. Phys. Chem.* **1992**, *96*, 3752.
(17) Clarke, D. L.; Oref, I.; Gilbert, R. G.; Lim, K. F. *J. Chem. Phys.* **1992**, *96*, 5983.
(18) Lendvay, G.; Schatz, G. C. *J. Chem. Phys.* **1992**, *96*, 4356.
(19) Bernshtein, V.; Oref, I. *J. Phys. Chem.* **1993**, *97*, 12811.
(20) Lendvay, G.; Schatz, G. C. *J. Chem. Phys.* **1993**, *98*, 1034.
(21) Bernshtein, V.; Oref, I. *J. Phys. Chem.* **1994**, *98*, 3782.
(22) Lim, K. F. *J. Chem. Phys.* (a) **1994**, *100*, 7385; (b) **1994**, *101*, 8756.
(23) Bernshtein, V.; Lim, K. F.; Oref, I. *J. Phys. Chem.* **1995**, *99*, 4531.
(24) Bernshtein, V.; Oref, I. *Chem. Phys. Lett.* **1995**, *233*, 173.
(25) Lenzer, T.; Luther, K.; Troe, J.; Gilbert, R. G.; Lim, K. F. *J. Chem. Phys.* **1995**, *103*, 626.
(26) Koifman, I.; Dashevskaya, E. I.; Nikitin, E. E.; Troe, J. *J. Phys. Chem.* **1995**, *99*, 15348.
(27) Clary, D. C.; Gilbert, R. G.; Bernshtein, V.; Oref, I. *Faraday Discuss.* **1995**, *102*.

(28) Bernshtein, V.; Oref, I. *J. Chem. Phys*. **1996**, *104*, 1958.
(29) Lendvay, G.; Schatz, G. C. *J. Phys. Chem.* **1994**, *98*, 6530.
(30) Rosenblum, I.; Dashevskaya, E. I.; Nikitin, E. E.; Oref, I. *Mol. Eng*. **1997**, *7*, 169.
(31) Bernshtein, V.; Oref, I. *J. Chem. Phys*. (a) **1998**, *108*, 3543; (b) **1998**, *109*, 9811.
(32) Venus, Quantum Chemistry Program Exchange by Hase, W. L.; Duchovic, R. J.; Hu, X.; Komornicki, A.; Lim, K. F.; Lu, D.-H.; Peslherbe, G. H.; Swamy, K. N.; Vande-Linde, S. R.; Varandas, A.; Wang, H.; Rolf, R. *J. Quantum Chem. Program Exchange Bull*. **1996**, *16* (4), 43 [QCPE Program 671].
(33) Bludsky, O.; Spirko, V.; Hrouda, V.; Hobza, P. *Chem. Phys. Lett*. **1992**, *196*, 410.
(34) Draeger, J. A. *Spectrochim. Acta*. **1985**, *41A*, 607.
(35) Kihara, T. *Rev. Mod. Phys*. **1953**, *25*, 831.
(36) Refson, K; Lie, G. C.; Clementi, E. *J. Chem. Phys*. **1987**, *87*, 3634.